Biomedical Optics EXPRESS

Correlative multicolor 3D SIM and STORM microscopy

Virginie Hamel,[1,3] Paul Guichard,[1,3] Mathias Fournier,[2,3] Romain Guiet,[2] Isabelle Flückiger,[1] Arne Seitz,[2] and Pierre Gönczy[1,*]

[1]*Swiss Institute for Experimental Cancer Research (ISREC), School of Life Sciences, Swiss Federal Institute of Technology (EPFL), Lausanne, Switzerland*

[2] *Bioimaging and Optics platform (BIOP), School of Life Sciences, Swiss Federal Institute of Technology (EPFL), Lausanne, Switzerland*

[3]*These authors contributed equally to this work*

[*]*Pierre.Gonczy@epfl.ch*

Abstract: Within the last decade, super-resolution methods that surpass the diffraction limit of light microscopy have provided invaluable insight into a variety of biological questions. Each of these approaches has inherent advantages and limitations, such that their combination is a powerful means to transform them into versatile tools for the life sciences. Here, we report the development of a combined SIM and STORM setup that maintains the optimal resolution of both methods and which is coupled to image registration to localize biological structures in 3D using multicolor labeling. We utilized this workflow to determine the localization of Bld12p/CrSAS-6 in purified basal bodies of *Chlamydomonas reinhardtii* with utmost precision, demonstrating its usefulness for accurate molecular mapping in 3D.

OCIS codes: (180.0180) Microscopy; (180.2520) Fluorescence microscopy; (180.6900) Three-dimensional microscopy; (100.6640) Superresolution; (170.3880) Medical and biomedical imaging.

References and links

1. A. Jost and R. Heintzmann, "Superresolution Multidimensional Imaging with Structured Illumination Microscopy," Annu. Rev. Mater. Res. **43**(1), 261–282 (2013).
2. M. G. L. Gustafsson, L. Shao, P. M. Carlton, C. J. R. Wang, I. N. Golubovskaya, W. Z. Cande, D. A. Agard, and J. W. Sedat, "Three-dimensional resolution doubling in wide field fluorescence microscopy by structured illumination," Biophys. J. **94**(12), 4957–4970 (2008).
3. B. Huang, W. Wang, M. Bates, and X. Zhuang, "Three-dimensional super-resolution imaging by stochastic optical reconstruction microscopy," Science **319**(5864), 810–813 (2008).
4. D. Kamiyama and B. Huang, "Development in the STORM," Dev. Cell **23**(6), 1103–1110 (2012).
5. S. Rossberger, G. Best, D. Baddeley, R. Heintzmann, U. Birk, S. Dithmar, and C. Cremer, "Combination of structured illumination and single molecule localization microscopy in one setup," J. Opt. **15**(9), 094003 (2013).
6. P. Thévenaz, U. E. Ruttimann, and M. Unser, "A pyramid approach to subpixel registration based on intensity," IEEE Trans. Image Process. **7**(1), 27–41 (1998).
7. P. Guichard, V. Hachet, N. Majubu, A. Neves, D. Demurtas, N. Olieric, I. Fluckiger, A. Yamada, K. Kihara, Y. Nishida, S. Moriya, M. O. Steinmetz, Y. Hongoh, and P. Gönczy, "Native architecture of the centriole proximal region reveals features underlying its 9-fold radial symmetry," Curr. Biol. **23**(17), 1620–1628 (2013).
8. N. Olivier, D. Keller, P. Gönczy, and S. Manley, "Resolution doubling in 3D STORM imaging through improved buffers," PLoS ONE **8**(7), e69004 (2013).
9. L. Blanchoin, R. Boujemaa-Paterski, C. Sykes, and J. Plastino, "Actin dynamics, architecture, and mechanics in cell motility," Physiol. Rev. **94**(1), 235–263 (2014).
10. Y. Nakazawa, M. Hiraki, R. Kamiya, and M. Hirono, "SAS-6 is a cartwheel protein that establishes the 9-fold symmetry of the centriole," Curr. Biol. **17**(24), 2169–2174 (2007).
11. P. Gönczy, "Towards a molecular architecture of centriole assembly," Nat. Rev. Mol. Cell Biol. **13**(7), 425–435 (2012).
12. D. Kitagawa, I. Vakonakis, N. Olieric, M. Hilbert, D. Keller, V. Olieric, M. Bortfeld, M. C. Erat, I. Flückiger, P. Gönczy, and M. O. Steinmetz, "Structural Basis of the 9-Fold Symmetry of Centrioles," Cell **144**(3), 364–375 (2011).
13. P. Guichard, A. Desfosses, A. Maheshwari, V. Hachet, C. Dietrich, A. Brune, T. Ishikawa, C. Sachse, and P. Gönczy, "Cartwheel Architecture of *Trichonympha* Basal Body," Science **337**(6094), 553 (2012).

#213625 - $15.00 USD Received 22 Aug 2014; revised 22 Aug 2014; accepted 22 Aug 2014; published 29 Aug 2014

14. D. Keller, M. Orpinell, N. Olivier, M. Wachsmuth, R. Mahen, R. Wyss, V. Hachet, J. Ellenberg, S. Manley, and P. Gönczy, "Mechanisms of HsSAS-6 assembly promoting centriole formation in human cells," J. Cell Biol. **204**(5), 697–712 (2014).
15. G. Piperno, M. LeDizet, and X. J. Chang, "Microtubules containing acetylated alpha-tubulin in mammalian cells in culture," J. Cell Biol. **104**(2), 289–302 (1987).
16. E. T. O'Toole and S. K. Dutcher, "Site-specific basal body duplication in Chlamydomonas," Cytoskeleton (Hoboken) **71**(2), 108–118 (2014).
17. Y.-W. Chang, S. Chen, E. I. Tocheva, A. Treuner-Lange, S. Löbach, L. Søgaard-Andersen, and G. J. Jensen, "Correlated cryogenic photoactivated localization microscopy and cryo-electron tomography," Nat. Methods **11**(7), 737–739 (2014).

1. Introduction

The development of super-resolution microscopy techniques has proven extremely powerful to localize proteins within a variety of biological samples with high precision. For instance, Structured Illumination Microscopy (SIM) can improve the resolution obtained by conventional confocal microscopy by a factor 2, yielding structural information at a resolution of ~120 nm in both X and Y axes [1,2]. Striking progress has also been achieved through Stochastic Optical Reconstruction Microscopy (STORM), which utilizes single molecule localization and reaches even higher spatial resolution, down to the 10 nm range [3]. However, STORM data can be difficult to interpret without clear structural information to place it into the cellular context. In this respect, the high-resolution structural information provided by SIM could be invaluable to interpret the STORM single molecule localization data. Moreover, because SIM and STORM can be subject to different kinds of artifacts during image reconstruction [1, 4], a combination of both techniques should help accurately interpret super-resolution data. Since both methods are based on wide field microscopy, they are particularly amenable to a combined approach. That this can be useful has been exemplified by a proof-of-principle study using a custom built microscope [5]. However, this setup did not implement the use of multicolor labeling or of 3D information, despite these modalities being critical for solving most biological questions. In this report, we describe a multicolor 3D correlative SIM and STORM microscopy workflow based on a commercial instrument coupled to image registration that provides a versatile means to accurately map proteins in their cellular context.

2. Materials and methods

2.1. Optical set-up

The combined SIM/STORM setup is based on the 3D NSIM/NSTORM Nikon microscope, utilizing a Nikon TI-E inverted microscope and a CFI Apochromat TIRF objective (100 x, NA 1.49, WD 0.12 mm). For SIM illumination, the light of a laser (Coherent Sapphire 488 nm, 200 mW or Coherent Sapphire 561 nm, 150 mW) is coupled into a multimodal fiber and the collimated output of the fiber directed onto a grating. Three diffraction orders (1 + ; 0; −1) are projected into the sample plane, forming the 3D-structured illumination pattern (thereafter called 3D SIM mode). The final image is reconstructed from 15 images (5 phase shifts and 3 rotations). In case of the 2D-SIM mode, the zero order is blocked and thus only two orders are used to form the 2D illumination pattern. In that case, 9 images (3 phase shifts ans 3 rotations) are sufficient to reconstruct the image. For STORM illumination, the light of a laser (MPBC 647 nm, 300 mW or Cobolt Jive 561 nm, 200 mW) is coupled into a single mode fibre and the collimated output focused (with the lens inside the TIRF condenser) onto the back focal plane of the objective to achieve either TIRF or inclined illumination.

SIM and STORM images are projected onto the chip of a back illuminated EM CCD camera (Andor iXON DU897). For SIM acquisitions, the acquisition time is set to 100 ms at a camera read out of 3 MHz. For STORM acquisitions, the chip is read out at 10 MHZ resulting in an exposure time of 16 ms for a field of view of 256 pixel by 256 pixel. The relay lens is selected depending on the imaging modality. A 2.5x lens is used for SIM imaging and a 1x lens for STORM imaging. Typically 5000-10000 frames are acquired during the STORM acquisition. In the case of 3D STORM imaging, a

#213625 - $15.00 USD Received 22 Aug 2014; revised 22 Aug 2014; accepted 22 Aug 2014; published 29 Aug 2014

cylindrical lens is used. Switching between the two modalities is easily feasible without touching the sample by moving the appropriate dichroic mirror in or out of the beam path. All elements are controlled with NIS Elements AR from Nikon.

2.2. Registration

STORM and SIM images are registered using the ImageJ plugin TurboReg that uses a pyramid approach for subpixel registration based on intensity [6]. The manual mode is used to align images by selecting similar structures detected in the SIM image and the corresponding STORM image. A bilinear mode is used to register images.

2.3. Immunofluorescence of mammalian cells

COS-7 and U2OS cells were grown in DMEM (Life Technologies) supplemented with 10% FBS and plated on a glass coverslip (Carl Roth, Cat No. LH 23.1, thickness 170µm). Cells were pre-extracted in CBS (10mM MES pH 6.9, 138mM KCl, 3mM $MgCl_2$ and 2mM EGTA) containing 0.2% NP-40 for 20 seconds and subsequently fixed in 3% paraformaldehyde and 0.1% glutaraldehyde for 15 minutes. Cells were permeabilized and blocked in PBS containing 0.2% Triton-X and 3% BSA for 1 hour.

For microtubule immunostaining, cells were incubated with primary antibodies against β-tubulin (mouse 1/500, Sigma, T4026) for one hour at room temperature, washed 5min in PBS and then for another hour at room temperature with secondary antibodies (goat anti-mouse Fab'2 AF647 1/1000, Life Technologies, A21237).

For non-muscle myosin, microtubules and F-actin triple immunostaining, cells were incubated first with Alexa Fluor 488 Phalloidin (165nM, Invitrogen) during the pre-extraction and blocking steps, and subsequently with primary antibodies against non-muscle myosin (rabbit 1/500, Polymyosin-A (MCH-A), Covance) and β-tubulin for one hour at room temperature, and then incubated for another hour at room temperature with the following secondary antibodies: goat anti-rabbit Fab'2 AF647 1/1000 (Life Technologies, A21246) and goat anti-mouse Fab'2 AF555 1/1000 (Life Technologies, A21425).

2.4. Bld12-Nterminus specific antibodies

HisBld12-NL(amino acids 1-503) and HisBld12-Nter(amino acids 1-159) proteins were produced using the *E. coli* strain BL21(DE3) (Stratagene). Bacteria were grown at 37°C to an $OD600_{nm}$ of approximately 0.5 in LB containing 40 µg/ml kanamycin. The temperature was switched to 20°C and the culture induced by adding isopropyl 1-thio-β-galactopyranoside (IPTG) to a final concentration of 1mM; protein expression was performed at 20°C for 16h. The resulting proteins were purified using Ni^{2+}-NTA Sepharose beads (GE Healthcare) at 4°C according to the manufacturer's instructions. Antibodies against Bld12p were raised against purified His-Bld12-NL(1-503) and injected into a rabbit (Eurogentec). Antibodies were subsequently strip-purified against Bld12-Nter(1-159), eluted with glycine pH 2.5 and neutralized with Tris-HCl pH 8.0.

2.5. Immunofluorescence microscopy of purified basal bodies

Isolated basal bodies were first purified [7] and centrifuged at 10,000 g onto a 12 mm diameter round coverslip (Thomas Scientific, coverslips #1.5, ref 1217N79) in a 15ml Corex tube containing special adaptors as described previously (Fisher, ref 4550015) and filled with 5ml 10mM K-PIPES, pH 7. Coverslips were then fixed for 7 min in –20°C methanol, washed in PBS, incubated 1 hr at room temperature with primary antibodies in 1% bovine serum albumin and 0.05% Triton X-100, washed 5 min in PBS, and incubated 1 hr at room temperature with secondary antibodies. Primary antibodies were 1:300 rabbit Bld12p-Nter and 1:1000 mouse acetylated tubulin (Sigma-Aldrich). Secondary antibodies were 1:1000 goat anti-rabbit coupled to Alexa 647 and 1:1000 goat anti-mouse coupled to Alexa 488.

From the raw SIM images, the corresponding wide field (WF) images were generated using a custom built ImageJ/Fiji macro that sums (or optionally averages) all the raw SIM images (all phases and orientations) for each slice and each channel. In order to enable

#213625 - $15.00 USD Received 22 Aug 2014; revised 22 Aug 2014; accepted 22 Aug 2014; published 29 Aug 2014

stringent comparison of SIM and WF images, the individual image was first normalized with respect to its own maximum and minimum intensity values, now corresponding to the percentage of their intensity histogram range. In a second step, the WF image was rescaled without interpolation to match the pixel size of the reconstructed SIM image. This allows identical ROI/line measurements for both imaging modalities.

Basal bodies were imaged in STORM buffer using an imaging chamber adapted for 12mm diameter coverslips (Harvard Apparatus, ref 69-1946). The STORM buffer contains 50 mM TRIS-HCl (pH 8.0), 10 mM NaCl, and 10% (w/v) Glucose. Immediately before imaging, the buffer was complemented with 2-Mercaptoethanol (final concentration 0.14 mol/l), glucose oxidase (final concentration 0.56 mg/ml) and catalase (final concentration 0.03 mg/ml).

3. Results

3.1. Image acquisition and reconstruction

In order to combine the advantages of SIM and STORM microscopy to accurately localize molecules within a given biological sample, we used a 3D commercial microscope, that provides both acquisition modes within one instrument (Fig. 1(A)-1(B)). This setup also permits the use of 3 laser excitations wavelength (488 nm, 561 nm and 640 nm) for the SIM module and of the 640 nm laser line for the STORM module, providing the system with multicolor image acquisition capability. Importantly, 3D imaging can be performed for both modes of super-resolution imaging. Moreover, this setup allows imaging of the same region of interest using SIM and STORM, ensuring direct comparison between the two resulting images. This is a prerequisite for efficient image registration and thus for placing the precise molecular localization provided by STORM into the structural context given by SIM.

In order to acquire such images, we prepared biological samples (fixed mammalian cells or purified basal bodies, see Materials and Methods) that were then immersed in a STORM buffer complemented with 2mM Cyclooctatetraene (COT) to enhance the blinking properties of the Alexa 647 fluorophore [8]. Given the high irradiance needed for STORM imaging, samples were first imaged using the SIM mode. Despite the different requirements of SIM and STORM imaging (very stable dye for SIM and blinking capability of the dye for STORM), the STORM COT buffer allowed suitable image acquisition in a single set-up. No blinking could be observed during the SIM acquisition for Alexa647, which is most probably explained with the much lower excitation intensity used. Following acquisition, reconstruction of the image was performed using the NIS software and saved for further analysis. We then switched to the STORM mode to image the same region of interest and reconstruct the resulting output (Fig. 1(C)).

#213625 - $15.00 USD Received 22 Aug 2014; revised 22 Aug 2014; accepted 22 Aug 2014; published 29 Aug 2014

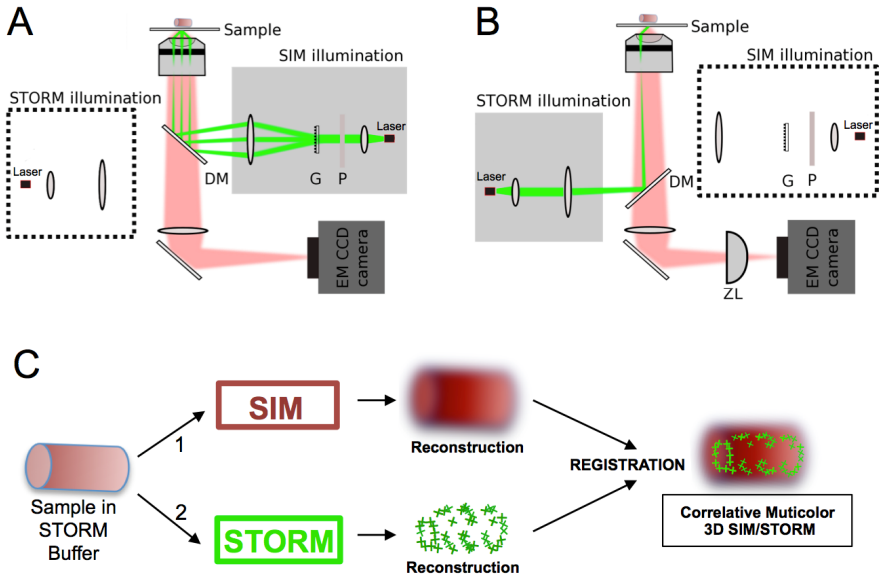

Fig. 1. Schematic of the microscope setup used for multicolor 3D correlative SIM/STORM imaging. The experiments were implemented on a Nikon TI-E inverted microscope. (A) To obtain structured illumination, a polarizer (P) and a diffraction grating (G) is used, which is suitable for creating a pattern for multiple wavelengths. (B) A classical TIRF illumination scheme was employed for the STORM experiment. Switching between the SIM and the STORM modalities can be easily realized by moving the dichroic mirrors (DM) in and out of the beam-paths. Both DMs are installed in the motorized filter turrets of the microscope. (C) Flow chart of the steps performed during image acquisition and processing to obtain a multicolor 3D correlative SIM/STORM image. Note that the SIM image (1) is taken before the STORM image (2).

3.2 SIM/STORM images registration

Once acquired and reconstructed, the SIM and STORM images need to be registered to allow a direct comparison of the same region of interest and generate a correlative SIM/STORM image (Fig. 1(C)). However, this is complicated because the reconstructed images differ in the field of view and pixel size. Indeed, due to the use of a 2.5x relay lens, the SIM images cover a smaller field of view and thus the STORM images need to be cropped to match this smaller size. Furthermore, the reconstructed SIM image (1024 pixel x 1024 pixel; 30 nm /pixel) must be scaled in order to match the dimensions of the cropped STORM image (4360 pixel x 4080 pixel; 8 nm/pixel) (Fig. 2(A)).

For further registration of the images, we used the ImageJ plugin TurboReg. Landmarks on both Source and Target images, corresponding to the SIM and the STORM reconstructed images, were selected manually. In order to preserve the high resolution provided by the STORM image, we used the STORM image as a reference, while the SIM image was scaled until the two could be overlaid (Fig. 2(B)).

#213625 - $15.00 USD Received 22 Aug 2014; revised 22 Aug 2014; accepted 22 Aug 2014; published 29 Aug 2014

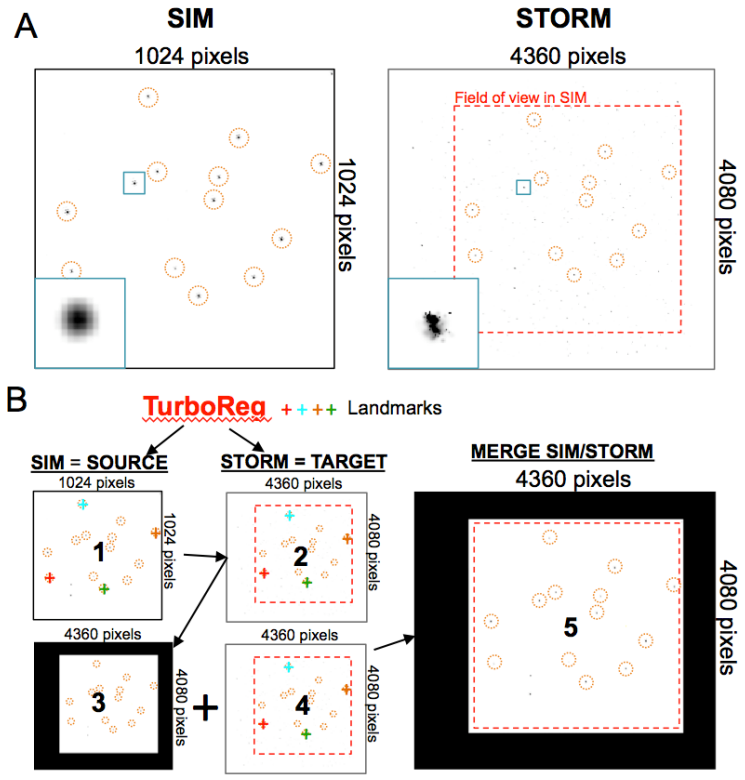

Fig. 2. Registration of SIM/STORM images (A) A region of interest containing Alexa-647nm-coupled beads of 40 nm in diameter was imaged successively in SIM and STORM. Note that the pixel size and field of view is smaller in SIM than it is in STORM. (B) The SIM and STORM images were registered onto one another using TurboReg. The SIM image (1) was used as SOURCE while the STORM image (2) served as TARGET. Landmarks were manually placed to select identical beads in both images, thus allowing the generation of a rescaled SIM image (3). The resulting image was then combined with the STORM image (4) to create an output image containing both SIM and STORM modalities (5).

In order to evaluate the quality of the images taken with this combined set-up, we imaged microtubules in COS-7 cells. Microtubules are polymeric assemblies composed of α and β-tubulin dimers that are important for many cellular processes. Each microtubule forms a polymer of 25 nm in outer diameter that cannot be resolved with standard microscopy techniques, as can be seen in Fig. 3(A) (wide field). Figure 3(B)-3(D) shows the same region imaged and then reconstructed in SIM (Fig. 3B) and STORM (Fig. 3(C)) modes.

We also measured the lateral plot profiles for the same microtubule for the three types of images (Fig. 3(E)). We found that the microtubule can be resolved to ~150 nm by SIM, whereas STORM allows one to resolve the inner space of microtubules to ~40 nm, consistent with a 25 nm structure enlarged by the antibodies (Fig. 3(F)). Importantly, the two reconstructed images can be registered onto one other (Fig. 3(D)), coupling the point localization information given by the STORM image onto the structural image provided by SIM. We conclude that this setup is compatible with data acquisition in combined SIM and STORM modes.

#213625 - $15.00 USD Received 22 Aug 2014; revised 22 Aug 2014; accepted 22 Aug 2014; published 29 Aug 2014

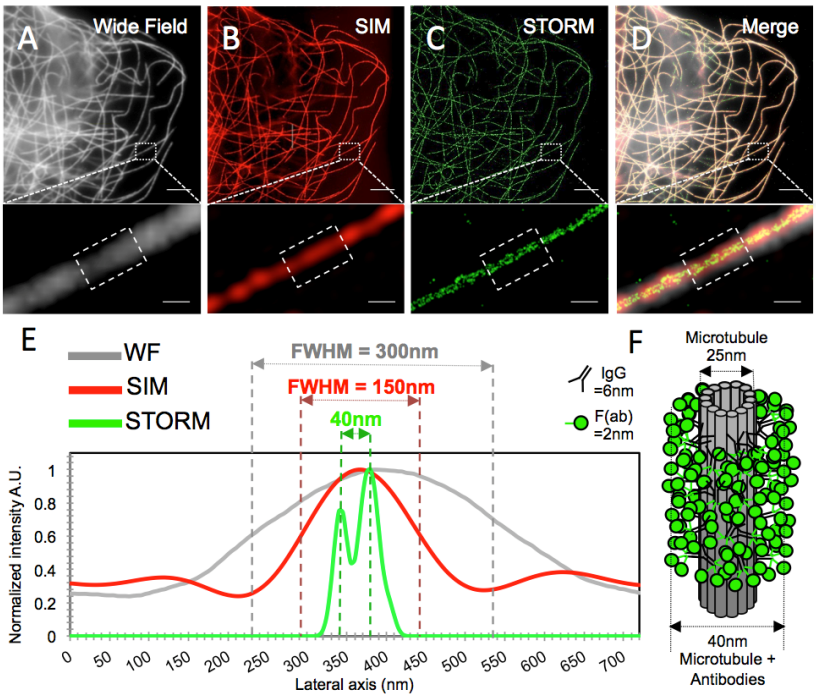

Fig. 3. 2D correlative SIM/STORM images. (A) Wide field, (B) SIM and (C) STORM images of microtubules in COS-7 cell. (D) Merge of the 3 images. Below each panel, a higher magnification view corresponding to the boxed region is shown. The scale bar corresponds to 100 nm. (E) Lateral plot profile of the different boxed regions with the corresponding full width at half maximum (FWHM). The values correspond to the average intensities along the microtubule inside the boxed regions. (F) Interpretation of result shown in D; schematic representation of a microtubule surrounded by antibodies.

3.2. Multicolor 2D imaging

Multicolor imaging is a prerequisite for detailed interrogation of biological samples. We hence assessed whether the workflow delineated above could be used in a multicolor mode. To this end, we triply stained U2OS cells to visualize the microtubule network, the F-actin network, and the molecular motor non-muscle myosin (hereafter referred to as myosin for simplicity), which generates force along F-actin filaments to power many cellular processes [9] (Fig. 4).

Actin was revealed using Alexa-488 conjugated phalloidin, and microtubules using primary antibodies directed against β-tubulin followed by secondary antibody fragments labeled with Alexa-555. Myosin was stained using primary antibodies against this protein followed by secondary antibody fragments labeled with Alexa-647, which is compatible with STORM imaging. We first acquired and reconstructed SIM images of F-actin (Fig. 4(A)), microtubules (Fig. 4(B)), and myosin (Fig. 4(C)) to obtain a structural pattern for each. The same region of interest was then acquired in STORM with Alexa-647 (Fig. 4(D)) to gain precise single molecular localization for myosin. Using TurboReg, we could overlay the multicolor information provided by the three individual SIM images (Fig. 4(F)), as well as merge the resulting multicolor SIM image with the myosin STORM image (Fig. 4(G), 4(E)). Importantly, myosin patches that are clearly detectable owing to the STORM mode could be placed back onto the F-actin network acquired by SIM, highlighting possible sites of interaction between myosin and F-actin (Fig. 4(F)-4(H)).

#213625 - $15.00 USD Received 22 Aug 2014; revised 22 Aug 2014; accepted 22 Aug 2014; published 29 Aug 2014

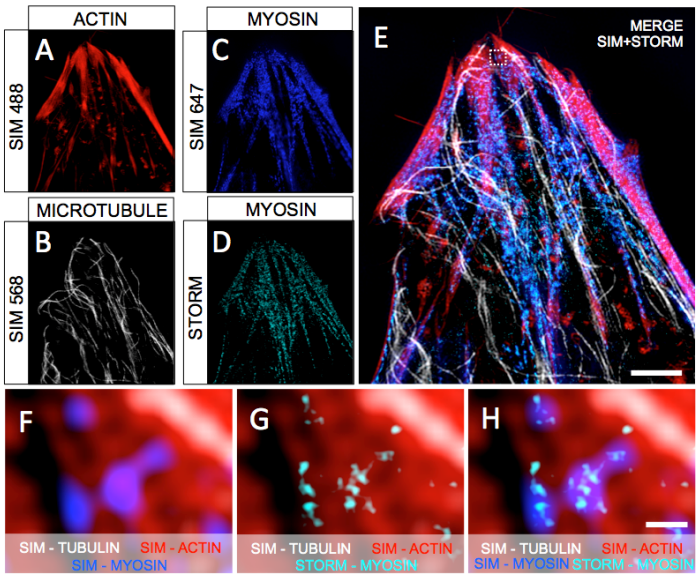

Fig. 4. Triple color correlative SIM/STORM imaging. (A-C) SIM images of U2OS cells stained for actin (A, red), microtubules (B, white) and non-muscle myosin (C, blue). (D) The same region of interest was imaged for non-muscle myosin in STORM (cyan). (E) Merge of the three SIM images with the non-muscle myosin STORM image. Scale bar: 2 µm. (F) Inset corresponding to the boxed region towards the top of (E) showing the merge of the three SIM images (actin, microtubules and non-muscle myosin). (G) Corresponding inset of the merge of the actin and microtubules SIM images with the non-muscle myosin STORM image, highlighting non-muscle myosin patches (cyan) decorating actin cables (red). (H) Corresponding inset of the merge of the three SIM images (actin, microtubule and non-muscle myosin), as well as the STORM image of non-muscle myosin. Scale bar: 200nm.

3.3. Multicolor 3D imaging of basal bodies

We sought to maximize the benefits of the combined SIM and STORM approach described above by implementing the 3D information present within both acquisition modes. We set out to utilize the power of this approach to investigate the distribution of Bld12p/CrSAS-6, a protein critical for formation of the basal body in the green alga *Chlamydomonas reinhardtii* [10]. Basal bodies are microtubule-based cylindrical organelles that are ~450 nm long and ~130 nm in inner diameter [11], dimensions that make them particularly well suited for such high-resolution imaging (Fig. 5(A)).

Basal body formation is seeded by a cartwheel that is ~100 nm high and comprises stacked slices of a structure that is characterized by a central hub ~22 nm in diameter, from which emanate nine radial spokes connecting to the peripheral microtubule triplets (Fig. 5(C), schematic top view). Bld12p is key for the formation of the cartwheel and localizes in the proximal region of the basal body as judged by electron microscopy and conventional light microscopy [10]. Bld12p forms ring-like structures *in vitro* that resemble a slice of the cartwheel observed *in vivo* [12]. Moreover, cryo-electron tomography revealed that the cartwheel in the flagellate *Trichonympha* could accommodate such ring-like structures [13]. Furthermore, STORM imaging using monoclonal antibodies recognizing the C-terminus of HsSAS-6 revealed that this part of the protein localizes towards the periphery of the cartwheel in human cells [14].

#213625 - $15.00 USD Received 22 Aug 2014; revised 22 Aug 2014; accepted 22 Aug 2014; published 29 Aug 2014

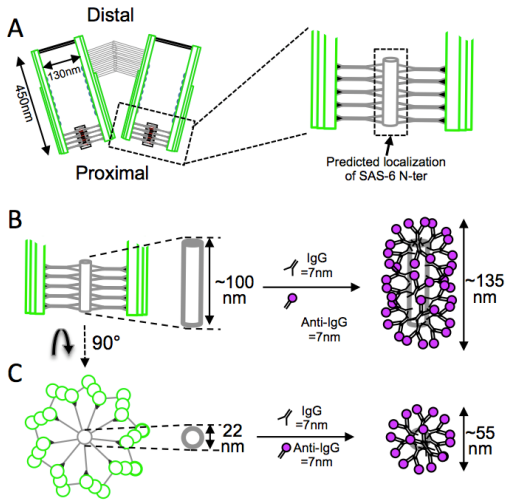

Fig. 5. Expected localization of the Bld12p N-terminus in *Chlamydomonas* basal body. (A) Schematic representation of a mature *Chlamydomonasi* basal body. The proximal region is boxed and enlarged on the right. The cartwheel is represented in grey and the microtubules in green. (B-C) Expected height and diameter of the cartwheel with and without decoration with antibodies in the longitudinal (B) or top view (C).

Despite these advances, a combined approach to accurately map in 3D the distribution of Bld12p, and in particular the N-terminus of the protein, is missing.

To address this question, we generated and purified antibodies that recognize the N-terminus of Bld12p (Materials and Methods). Given the dimensions of the primary and secondary antibodies, and provided optimal imaging, we expect the fluorescent signal corresponding to Bld12-Nter to be ~135 nm high and ~55 nm in diameter (Fig. 5(B)-5(C)). We stained purified *Chlamydomonas* basal bodies with primary antibodies against Bld12p Nter, together with antibodies against acetylated tubulin, which marks the microtubules of basal bodies [15]. As shown in a representative image (Fig. 6), wide field and 3D SIM imaging established that Bld12p is located in the proximal region of the basal body, as expected for a cartwheel protein [10]. However, the low axial resolution in SIM imaging did not allow us to properly resolve the architecture of Bld12p assemblies. This is illustrated by the fact that the decorated cartwheel is 397nm thick whereas estimated dimensions is ~55nm (Fig. 6(F)-6(G) and Fig. 5(B)-5(C)).

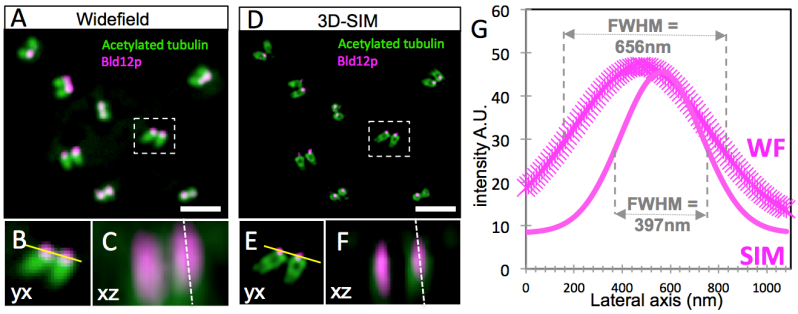

Fig. 6. Comparison of axial resolution between wide field (WF) and SIM images. (A) WF image of purified *Chlamydomonas* basal bodies stained for acetylated tubulin (green) and Bld12p N-terminal specific antibody (magenta). (B, C) Inset of basal bodies; yx lateral view (B) and xz axial view (C) along the line shown in (B). (D) SIM image of purified *Chlamydomonas* basal bodies stained for acetylated tubulin (green) and with Bld12p N-terminal specific antibody (magenta). (E, F) Inset of basal bodies; yx lateral view (E) and xz axial view (F) along the line shown in (E). (G) Plot profile of the lines shown in (C) and (F). The FWHM indicate a resolution of about 700nm in WF and 400nm in 3D SIM. Scale bar: 2 microns.

#213625 - $15.00 USD Received 22 Aug 2014; revised 22 Aug 2014; accepted 22 Aug 2014; published 29 Aug 2014

Then we imaged such basal bodies using the combined SIM and STORM approach to achieve precise localization of Bld12p.

As shown in Fig. 7(C)-7(D), we could image and register the STORM data onto the SIM volume. Using the 3D STORM data (Fig. 7(E)), we found that the Bld12 signal in the two displayed basal bodies covers ~110 nm and ~160 nm in height and ~41nm and ~52nm in diameter, within the range of expected dimensions for the cartwheel (see Fig. 5(B)-5(C)). These measurements are consistent with a recent report showing that the cartwheel in *Chlamydomonas* is a dynamic structure, with sizes ranging between 42 nm and 163 nm in height as judged by electron tomography [16].

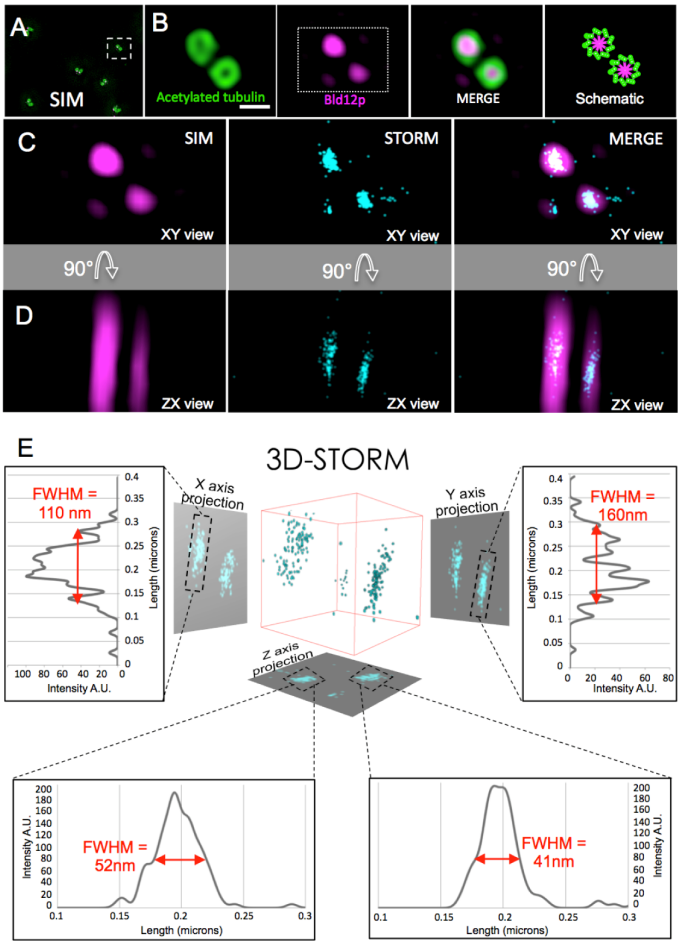

Fig. 7. Precise 3D mapping of Bld12p in purified basal bodies. (A) 3D SIM image of purified basal bodies reconstructed from 15 images (3 phases, 3 rotations) stained for acetylated tubulin (green) and with Bld12p N-terminal specific antibody (magenta). Scale bar: 500nm. (B) Insets of select basal bodies (corresponding to the boxed regions in panel A). The panels on the right provide a schematic representation of the observed structures. Scale bars: 200nm. Note that the Bld12p-Nter is located at the base and in the center of the basal bodies. (C, D) 3D SIM and STORM images of Bld12p-Nter in x, y (D) and z, x views (E). Note the gain in resolution for mapping the position of the Bld12p. (E) 3D STORM data for Bld12p N-terminus from the pair of basal bodies shown in C, with their projections onto the indicated axes, as well as plot profiles of the corresponding intensity projections.

4. Conclusion and outlook

In this paper, we report a simple workflow for multicolor 3D correlative imaging combining SIM and STORM as a powerful means to provide topological information

#213625 - $15.00 USD Received 22 Aug 2014; revised 22 Aug 2014; accepted 22 Aug 2014; published 29 Aug 2014

(SIM) coupled with single molecule localization (STORM). Importantly, we could maintain the optimal resolution of SIM and STORM using a similar buffer supplemented with COT. Moreover, we used image registration to localize biological structures in 3D with multicolor labeling. The gain of information provided by this combined set up is expected to help resolve important biological questions by precisely mapping protein localization onto complex structures. We exemplified the power of this approach here by resolving the precise 3D localization of the key cartwheel component Bld12p in purified basal bodies from *Chlamydomonas*.

The development of methods to accurately localize proteins within their cellular context can be achieved through different routes, such as the one described in this paper, or else through the combination of super-resolution and cryo-electron microscopy. This novel method enables native structural information provided by cryo-electron microscopy to be combined with STORM single molecule localization [17]. One significant advance for the future would be to combine SIM, STORM and cryo-electron microscopy in multicolor imaging to push even further the localization precision of given proteins within their biological context.

Acknowledgments

We thank Suliana Manley and Fernando R. Balestra for critical reading of the manuscript. Pa.G. held a postdoctoral fellowship from EMBO (ALTF 286-2011). This work was also supported by the ERC (AdG 233335 to Pi.G.).

#213625 - $15.00 USD Received 22 Aug 2014; revised 22 Aug 2014; accepted 22 Aug 2014; published 29 Aug 2014